European Review for Medical and Pharmacological Sciences 2020; 24: 12001-12008

MiR-182 inhibits oxidative stress and epithelial cell apoptosis in lens of cataract rats through PI3K/Akt signaling pathway

L. YAO, H. YAN

Department of Ophthalmology, Tianjin Medical University General Hospital, Tianjin, China

Abstract. – OBJECTIVE: The aim of this study was to investigate the influences of micro ribonucleic acid (miR)-182 on oxidative stress and epithelial cell apoptosis in the lens of cataract rats through the phosphatidylinositol 3-hydroxy kinase/protein kinase B (PI3K/Akt) pathway.

MATERIALS AND METHODS: A total of 36 Sprague-Dawley rats were randomly assigned into three groups, including normal group (n=12), model group (n=12), and miR-182 mimics group (n=12). Rats in normal group were first normally fed. After establishing the cataract model, rats in model group were intraperitoneally injected with normal saline. Meanwhile, rats in miR-182 mimics group were intraperitoneally injected with miR-182 mimics. At 7 d after operation, materials were sampled. The expressions of B-cell lymphoma 2 (Bcl-2) and Bcl-2 associated X protein (Bax) were detected via immunofluorescence. The protein expressions of PI3K and Akt were detected using Western blotting. Moreover, the expression level of miR-182 was measured via qPCR. Cell apoptosis was evaluated using terminal deoxynucleotidyl transferase (TdT) dUTP nick-end labeling (TUNEL). In addition, the content of superoxide dismutase (SOD) and malondialdehyde (MDA) was determined using enzyme-linked immunosorbent assay (ELISA).

RESULTS: Compared with normal group, both model group and miR-182 mimics group exhibited significantly up-regulated expression level of Bax and down-regulated expression of Bcl-2 ($p<0.05$). MiR-182 mimics group had markedly lower expression level of Bax and higher expression level of Bcl-2 than model group ($p<0.05$). Western blotting results demonstrated that the protein expression levels of PI3K and Akt in model and miR-182 mimics groups were considerably higher than those in normal group ($p<0.05$). Meanwhile, their protein expression levels in miR-182 mimics group were significantly higher than those in model group ($p<0.05$). In comparison with normal group, the expression level of miR-182 was markedly up-regulated in both model group and miR-182 mimics group ($p<0.05$). Moreover, its expression level in miR-182 mimics group was considerably higher than that in model group ($p<0.05$). TUNEL-positive cells increased significantly in both model group and miR-182 mimics group when compared with normal group ($p<0.05$). However, they were remarkably reduced in miR-182 mimics group when compared with model group ($p<0.05$). Compared with normal group, model and miR-182 groups exhibited substantially decreased SOD content and increased MDA content ($p<0.05$).

CONCLUSIONS: MiR-182 inhibits oxidative stress and epithelial cell apoptosis in the lens of cataract rats by activating the PI3K/Akt signaling pathway.

Key Words:
Cataract, PI3K/Akt signaling pathway, MiR-182, Apoptosis, Oxidative stress.

Introduction

Cataract, a clinically common ocular disease, frequently occurs in the elderly. Since it tends to cause blindness of patients, cataract is considered one of the major blinding diseases in humans[1,2]. Some studies[3,4] have argued that chronic oxidative stress response induced by the synergy of multiple factors, including genetics, aging, nutrition, radiation, and immunity and metabolism abnormalities, is one of the main pathological mechanisms of cataract. Persistent damage caused by long-standing chronic oxidative stress responses in the eye to lens epithelial cells can eventually lead to the apoptosis and necrosis of lens epithelial cells and other pathological reactions. Furthermore, this may impair normal physiological functions of the lens, thereby inducing cataract. The leading manifestations of cataract in patients include *muscae volitantes*, blurred vision, and even blindness, seriously endangering human health.

Corresponding Author: Hua Yan, MD; e-mail: yaoling1518647581@163.com

As an important member of the micro ribonucleic acid (miRNA) family, miR-182 plays a crucial role in pathophysiological processes such as cell proliferation and apoptosis by modulating the activation of several downstream signaling pathways and expressions of various effector molecules. MiR-182 plays an important role in congenital cataract, glaucoma, and retinal dysfunctions[5-7]. The phosphatidylinositol 3-hydroxy kinase/protein kinase B (PI3K/Akt) pathway signaling pathway is a vital cellular signaling pathway. It has been confirmed to be closely related to oxidative stress responses and cell apoptosis. Under the stimulation of various cytokines, the PI3K/Akt signaling pathway is activated due to the phosphorylation of Akt[8]. This can exert important anti-oxidative stress response and anti-apoptosis effects and down-regulate the multiple downstream effector molecules, eventually reducing damage to cells, tissues, and organisms[9].

Therefore, the aim of the present study was to investigate the influences of miR-182 on oxidative stress and epithelial cell apoptosis in the lens of cataract rats to further elucidate the underlying mechanism.

Materials and Methods

Laboratory Animals and Grouping

A total of 36 female Sprague-Dawley rats weighing (200±10) g were randomly divided into three groups, including normal group (n=12), model group (n=12), and miR-182 mimics group (n=12). All rats were raised in the Laboratory Animal Center, with free access to purified water and adequate feed daily, as well as 12/12 h light-dark cycle. This study was approved by the Laboratory Animal Ethics Committee of Tianjin Medical University General Hospital.

Main Reagents

MiR-182 mimics (Boster, Wuhan, China), anti-B-cell lymphoma 2 (Bcl-2) antibody, anti-Bcl-2 associated X protein (Bax) antibody, anti-PI3K and anti-phosphorylated Akt (p-Akt) antibody (Abcam, Cambridge, MA, USA), immunofluorescence and terminal deoxynucleotidyl transferase-mediated dUTP nick end labeling (TUNEL) kits (Fuzhou Maxim Biotech Co., Ltd., Fuzhou, China), AceQ quantitative polymerase chain reaction (qPCR) SYBR Green Master Mix kit and HiScript II Q RT SuperMix for qPCR [+genomic deoxyribonucleic acid (+gDNA) wiper] kit (Vazyme Biotech, Nanjing, China), optical microscope (Leica DMI 4000B/DFC425C, Wetzlar, Germany), and fluorescence qPCR instrument (ABI 7500, Applied Biosystems, Foster City, CA, USA).

Modeling and Treatment in Each Group

The rat cataract model was prepared using ultraviolet radiation specifically as follows: mydriatics was dripped into both eyes of rats, and the pupils of rats were observed 5 min later. When the pupils were confirmed completely dilated, the rats were fixed on a fixing plate, followed by persistent radiation for 15 min under ultraviolet light twice daily. Upon completion of radiation, the rats were transferred into cages and normally fed. Finally, the rat cataract model of could be established after persistent radiation for 15 d.

Rats in normal group were normally fed with normal diet and purified water daily, without any treatment. After the successful establishment of cataract model, rats in model group were fed with normal diet and purified water daily. Next, they were intraperitoneally injected with normal saline once a day. Meanwhile, rats in miR-182 mimics group were injected with miR-182 mimics using a micro-injector. After continuous intervention for 7 d, all rats were sacrificed for sampling.

Sampling

After anesthesia, 6 rats in each group were fixed using paraformaldehyde perfused. Lens tissues were taken out when the limbs of rats became stiff. Next, the tissues were soaked in paraformaldehyde and fixed for another 48 h. The remaining 6 rats in each group were used for direct removal of lens tissues. Harvested lens tissues were placed in Eppendorf (EP) tubes and stored in an ultra-low temperature refrigerator for later use.

Immunofluoroscence

Pre-paraffin-embedded tissues were first sliced into 5 μm-thick sections. Then, the tissues were extended in warm water at 42°C, mounted, baked, and prepared into paraffin-embedded tissue sections. Subsequently, paraffin-embedded tissue sections were soaked in xylene solution and gradient ethanol successively for deparaffinization and hydration. Next, the resulting sections were immersed in citrate buffer and heated for

3 min and braised for 5 min for 3 times using a micro-wave oven for complete antigen retrieval. After rinsing, the sections were added dropwise with endogenous peroxidase blocker, reacted for 10 min, rinsed, and sealed using goat serum in drops for 20 min. After discarding the goat serum blocking solution, the sections were incubated with primary antibodies (1:200) of anti-Bax and anti-Bcl-2 in a refrigerator at 4°C overnight. On the next day, the sections were rinsed and added dropwise with corresponding secondary antibody solution, followed by reaction for 10 min. After fully rinsing, the sections were reacted with streptomycin avidin-peroxidase solution for 10 min and added with DAB in drops for color development. Cell nuclei were counterstained with hematoxylin. Finally, the sections were sealed and observed.

Western Blotting

Cryopreserved lens tissues were added with lysis buffer, bathed on ice for 1 h, and centrifuged at 14,000 g for 10 min. Extracted protein was quantified by the bicinchoninic acid (BCA) method (Pierce, Rockford, IL, USA). Protein concentration was calculated based on the absorbance measured using a micro-plate reader and the standard curve. Subsequently, total proteins were denaturalized and isolated *via* sodium dodecyl sulphate-polyacrylamide gel electrophoresis (SDS-PAGE) that was terminated when it was observed that the marker protein was located at the bottom of a glass plate in a straight line. Next, the proteins were transferred onto polyvinylidene difluoride (PVDF) membranes (Millipore, Billerica, MA, USA). After sealing for 1.5 h, the membranes were incubated with primary antibodies of anti-PI3K, anti-p-Akt (1:1,000) overnight. After rinsing, the membranes were incubated with corresponding secondary antibodies (1:1,000). Immunoreactive bands were finally exposed by the enhanced chemiluminescence (ECL) method.

QPCR

Total RNA in stored lens tissues were extracted using TRIzol reagent. Subsequently, extracted RNAs were reversely transcribed into complementary deoxyribose nucleic acids (cDNAs) using the transcription kit. QPCR was performed in a 20 μL system under the following conditions: reaction at 53°C for 5 min, pre-denaturation at 95°C for 10 min, denaturation at 95°C for 10s and annealing at 62°C for 30 s, for a total of 30 cycles. After the value of ΔCt was calculated, the differences in the expression of target genes were analyzed. Primer sequences used in this study were shown in Table I.

TUNEL Assay

Tissues embedded in paraffin in advance were made into 5 μm-thick sections. The tissues were extended in warm water at 42°C, mounted and baked, and prepared into paraffin-embedded tissue sections. Subsequently, the sections were routinely de-paraffinized and hydrated by immersing in xylene solution and gradient ethanol successively. Next, the sections were added dropwise with TdT reaction solution, followed by reaction in the dark for 1 h. The reaction was stopped through incubation with deionized water in drops for 15 min. Then, the activity of endogenous peroxidase was blocked by hydrogen peroxide in drops. The sections were added dropwise with working solution, reacted for 1 h, rinsed, added with diaminobenzidine (DAB) solution in drops for color development, and rinsed again. Finally, the sections were sealed and observed.

Detection of Oxidative Stress-Associated Molecules Superoxide Dismutase (SOD) and Malondialdehyde (MDA) Using Enzyme-Linked Immunosorbent Assay (ELISA)

Fresh lens tissues were fully ground into minced ones in a grinder. According to the instructions of the ELISA kit, the samples and standard were separately loaded into a plate, added

Table I. List of primer sequences.

Name	Primer sequences
MiR-182	Forward: 5' GTGGCATTACATAGTCAGCA 3' Reverse: 5' GTGCAGGGTCCGAGGT 3'
GAPDH	Forward: 5' ACGGCAAGTTCAACGGCACAG 3' Reverse: 5' GAAGACGCCAGTAGACTCCACGAC 3'

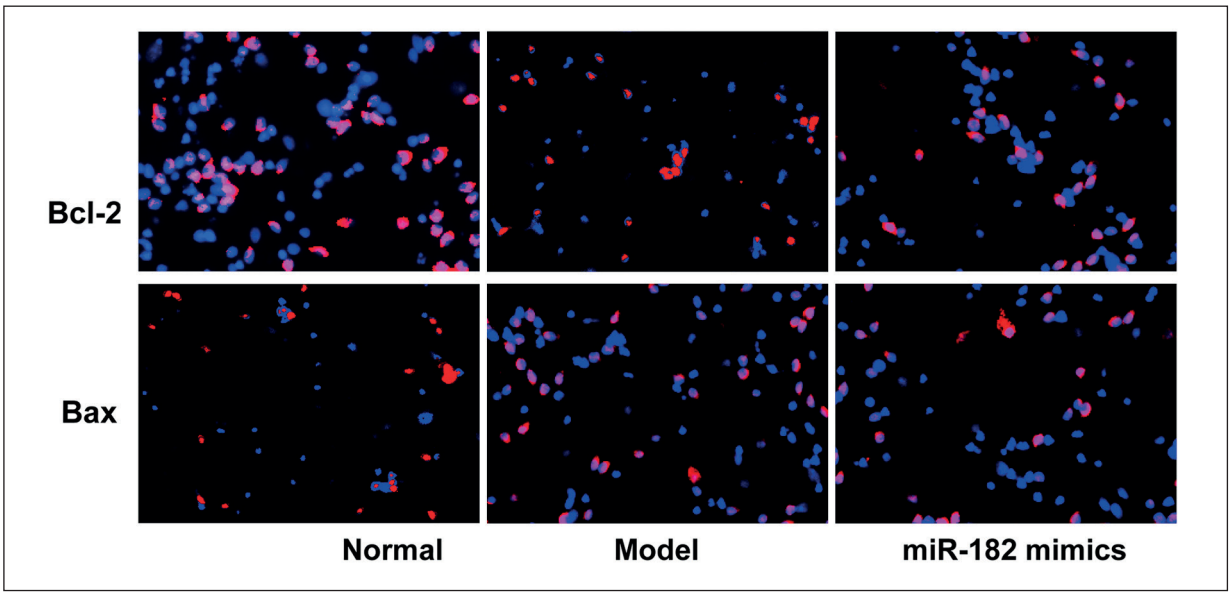

Figure 1. Expressions of Bax and Bcl-2 detected *via* immunofluorescence staining (magnification: 400×).

with biotinylated antibody working solution and enzyme-conjugated substance working solution. Then, the plate was washed. Finally, the products at 450 nm were detected by a micro-plate reader.

Statistical Analysis

Statistical Product and Service Solutions (SPSS) 20.0 software (IBM, Armonk, NY, USA) was employed for all statistical analysis. The *t*-test, corrected *t*-test, and nonparametric test were performed for data conforming to normal distribution and homogeneity of variance, those conforming to normal distribution and heterogeneity of variance, and those dissatisfying normal distribution and homogeneity of variance, respectively. One-way ANOVA test was used for pairwise comparisons followed by Post-Hoc Test (Least Significant Difference). Rank sum test was used for ranked data, and chi-square test was adopted for enumeration data. $p<0.05$ was considered statistically significant.

Results

Expressions of Bax and Bcl-2 Detected Via immunofluorescence

As shown in Figure 1, Bax-positive and Bcl-2-positive cells were tan. Normal group had few Bax-positive cells, but more Bcl-2-positive cells. However, both model and miR-182 mimics groups showed more Bax-positive cells and fewer Bcl-2-positive cells. According to the statistical results (Figure 2), compared with normal group, the average optical density of Bax-positive cells rose substantially, whereas that of Bcl-2-positive cells was notably lowered in model and miR-182 mimics groups, showing statistically significant differences ($p<0.05$). However, miR-182 mimics group exhibited evidently lower average optical density of Bax-positive cells and higher average optical density of Bcl-2-positive cells than model group, with statistically significant differences ($p<0.05$).

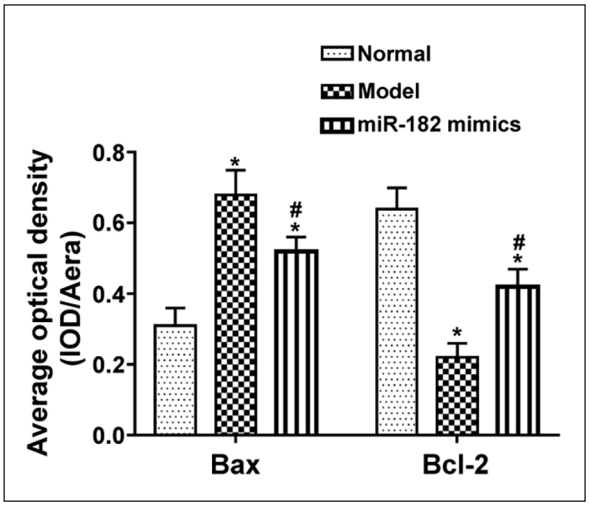

Figure 2. Average optical density of Bcl-2- and Bax-positive cells in each group. Note: $^{*}p<0.05$ *vs.* normal group, and $^{\#}p<0.05$ *vs.* model group.

Western Blotting Results

The protein expression levels of PI3K and p-Akt in normal group were significantly lower than the other two groups (p<0.05, Figure 3). Statistical results revealed that the relative protein expression levels of PI3K and p-Akt were substantially elevated in model and miR-182 mimics groups when compared with normal group, and the differences were statistically significant (p<0.05). Conversely, the relative protein expression levels of PI3K and p-Akt in miR-182 mimics group were markedly lower than those in model group (p<0.05) (Figure 4).

QPCR Results

In comparison with normal group, the relative expression level of miR-182 was markedly up-regulated in the other two groups, with statistically significant differences (p<0.05). Meanwhile, its relative expression level in miR-182 mimics group was remarkably higher than that of model group (p<0.05) (Figure 5).

Cell Apoptosis Rate Measured Via TUNEL Assay

As shown in Figure 6, apoptotic cells were tan. Normal group had fewer such cells than the other two groups. Compared with normal group, the other two groups exhibited substantially increased average optical density of TUNEL-positive apoptotic cells, showing statistically significant differences (p<0.05). Moreover, the average optical density in miR-182 mimics group was notably lower than model group, with a statistically significant difference (p<0.05) (Figure 7).

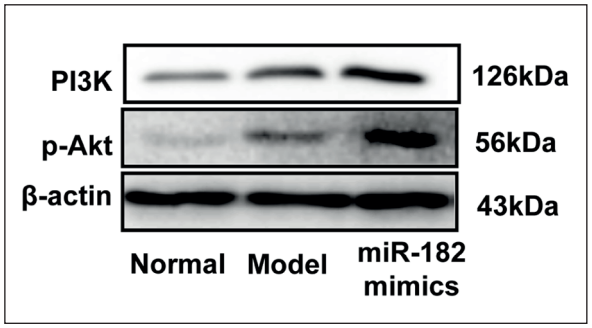

Figure 3. Expressions of related proteins detected *via* Western blotting.

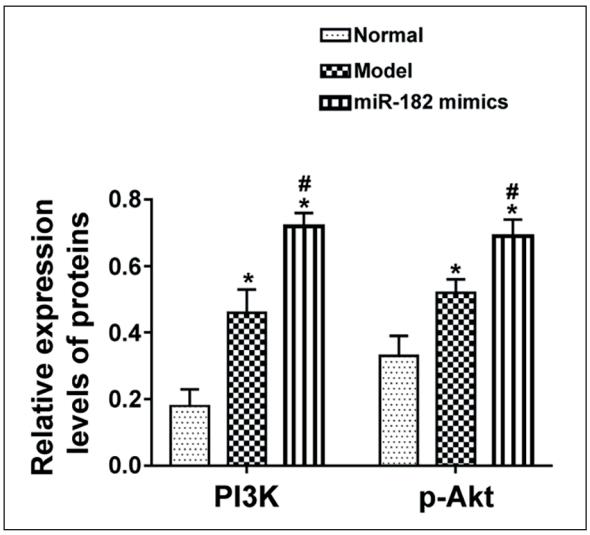

Figure 4. Relative expression levels of proteins in each group. Note: *p<0.05 *vs.* normal group, and #p<0.05 *vs.* model group.

Content of Oxidative Stress-Associated Molecule MDA and Anti-Oxidative Stress-Associated Molecule SOD

Compared with normal group, the content of oxidative stress-associated molecule MDA rose considerably, while that of anti-oxidative stress molecule SOD declined notably in model and miR-182 mimics groups, displaying statistically significant differences (p<0.05). In addition, miR-182 mimics group exhibited remarkably lower MDA content and higher SOD content than model group (p<0.05) (Figure 8).

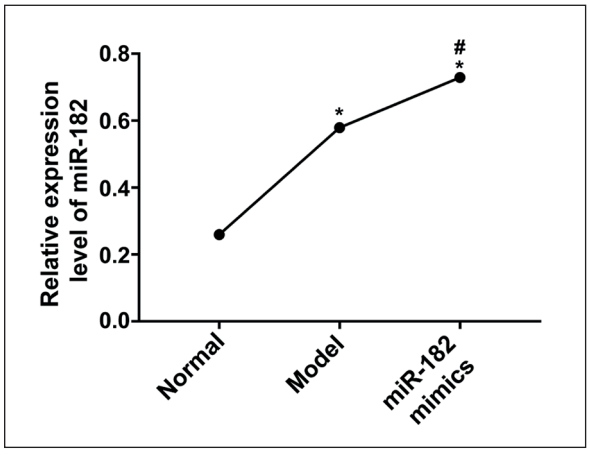

Figure 5. Relative expression level of miR-182 in each group. Note: *p<0.05 *vs.* normal group, and #p<0.05 *vs.* model group.

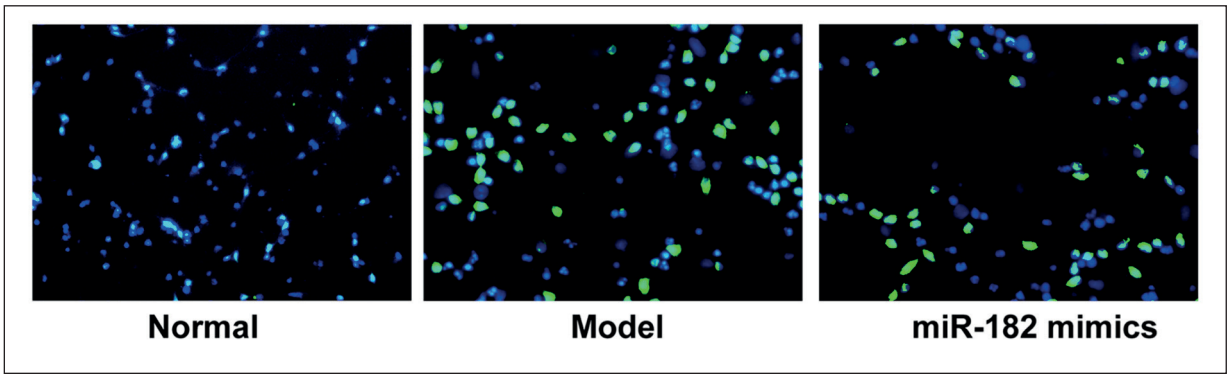

Figure 6. Cell apoptosis detected *via* TUNEL assay (magnification: 400×).

Discussion

Some studies[10,11] have demonstrated that oxidative stress responses and oxidative stress response-induced lens epithelial cell apoptosis are the primary pathological mechanisms for the onset of cataract. Persistent oxidative stress responses can change the structure and function of lens epithelial cells, eventually affecting the function of lens and resulting in relevant symptoms. Influenced by a variety of factors, the injury-induced release of manifold cytokines activates the signaling pathways related to oxidative stress response and apoptosis in lens epithelial cells. This can result in a substantial increase in the content of oxidative stress response-associated molecules such as MDA and a notable decline in that of anti-oxidative stress response-associated molecules as SOD[12,13]. Sustained high-intensity oxidative stress responses can further activate cell apoptosis-associated pathways and lead to abnormalities in the expressions of downstream effector molecules, including Bax and Bcl-2. Ultimately, this can induce cell apoptosis. Recently, it has been corroborated that[14,15] injuries, cytokines, and inflammatory factors contribute to the aberrantly high expression of pro-apoptosis molecule Bax, as well as the abnormally low expression of anti-apoptosis molecule Bcl-2. Both molecules act on the downstream apoptosis-associated effectors, ultimately resulting in the worsening of neuronal apoptosis[16,17]. According to the results of this study, the lens of cataract rats had abnormally highly expressed pro-apoptosis molecule Bax and pro-oxidative stress response-associated molecule MDA, as well as aberrantly

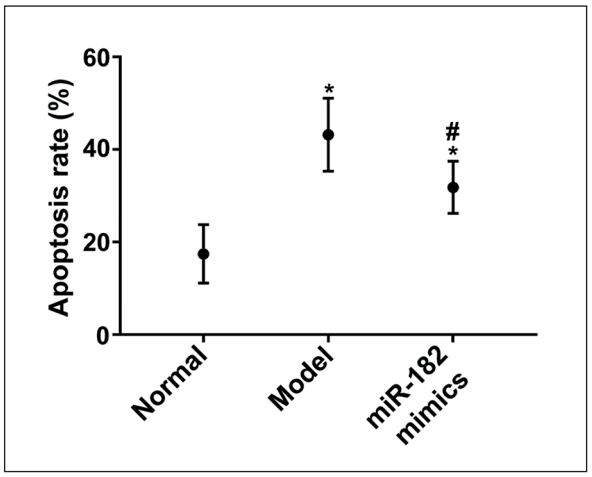

Figure 7. Apoptosis rate in each group. Note: **p*<0.05 *vs.* normal group, and #*p*<0.05 *vs.* model group.

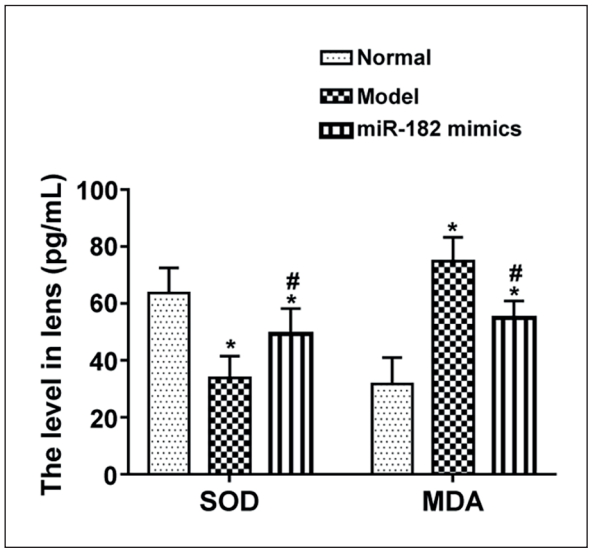

Figure 8. Content of SOD and MDA in lens in each group. Note: **p*<0.05 *vs.* normal group, and #*p*<0.05 *vs.* model group.

lowly expressed anti-apoptosis molecule Bcl-2 and anti-oxidative stress response molecule SOD. Our findings suggested that oxidative stress response and cell apoptosis occurred in the lens of cataract rats. Therefore, it is of great significance to effectively regulate oxidative stress response and cell apoptosis in lens epithelial cells for the treatment of cataract.

The PI3K/Akt signaling pathway is an important cellular signal transduction pathway[18,19]. It serves as a crucial mediator in multiple processes, such as cell proliferation, apoptosis, necrosis, and oxidative stress responses. PI3K/Akt signaling pathway is a canonical anti-oxidative stress and anti-apoptosis pathway[20]. It can effectively attenuate post-injury oxidative stress responses and apoptosis, thereby exerting a protective effect. Wang et al[21] have found that after injury, intracellular PI3K can be activated to form massive inositol triphosphates. As the secondary messenger, inositol triphosphates are able to further activate and phosphorylate Akt to produce p-Akt. This may transduce signals to modulate the gene transcription of the downstream Bax and Bcl-2 and their protein translation and expressions, as well as the expressions of downstream oxidative stress response-associated MDA and SOD[22,23]. Ultimately, oxidative stress responses and apoptosis are inhibited.

MiR-182, one of the crucial miRNA family members, regulates the physiological and pathological responses including cell proliferation and apoptosis. MiR-182 has been found[24-26] to exert important anti-oxidative stress and anti-apoptosis effects. It can effectively reduce cell apoptosis after injuries to protect damaged tissues and cells[24-26]. Based on the findings in this study, Bax and MDA were abnormally highly expressed, while Bcl-2 and SOD were aberrantly lowly expressed in the lens of cataract rats. These findings implied that high levels of oxidative stress response and cell apoptosis occurred in lens tissues. TUNEL assay verified that the lens epithelial cell apoptosis was significantly aggravated. Besides, miR-182 mimics effectively repressed the expressions of Bax and MDA, whereas up-regulated those of Bcl-2 and SOD, thereby reducing the levels of oxidative stress response and cell apoptosis. Western blotting results indicated that in the lens of cataract rats, the levels of p-PI3K and p-Akt were significantly elevated. Moreover, the PI3K/Akt signaling pathway was activated due to the self-protection mechanism in organisms to resist oxidative stress and apoptosis. However, miR-182 mimics further promoted the phosphorylation of Akt to up-regulate the expression of the PI3K/Akt signaling pathway. Therefore, it could be concluded that miR-182 activated the PI3K/Akt signaling pathway to inhibit oxidative stress and epithelial cell apoptosis in the lens of cataract rats.

Conclusions

In summary, we first detected that miR-182 inhibits oxidative stress and epithelial cell apoptosis in the lens of cataract rats by activating the PI3K/Akt signaling pathway. We could provide a potential strategy for the treatment of cataract in future.

Conflict of Interest

The Authors declare that they have no conflict of interests.

References

1) Simunovic M, Paradzik M, Skrabic R, Unic I, Bucan K, Skrabic V. Cataract as early ocular complication in children and adolescents with Type 1 diabetes mellitus. Int J Endocrinol 2018; 2018: 6763586.
2) Kamiya K, Iijima K, Nobuyuki S, Mori Y, Miyata K, Yamaguchi T, Shimazaki J, Watanabe S, Maeda N. Predictability of intraocular lens power calculation for cataract with keratoconus: a multicenter study. Sci Rep 2018; 8: 1312.
3) Zhao WJ, Yan YB. Increasing susceptibility to oxidative stress by cataract-causing crystallin mutations. Int J Biol Macromol 2018; 108: 665-673.
4) Ottonello S, Foroni C, Carta A, Petrucco S, Maraini G. Oxidative stress and age-related cataract. Ophthalmologica 2000; 214: 78-85.
5) Wu CR, Ye M, Qin L, Yin Y, Pei C. Expression of lens-related microRNAs in transparent infant lenses and congenital cataract. Int J Ophthalmol 2017; 10: 361-365
6) Liu S, Lin Y, Liu X. Meta-analysis of association of obstructive sleep apnea with glaucoma. J Glaucoma 2016; 25: 1-7.
7) Wu KC, Chen XJ, Jin GH, Wang XY, Yang DD, Li YP, Xiang L, Zhang BW, Zhou GH, Zhang CJ, Jin ZB. Deletion of miR-182 leads to retinal dysfunction in mice. Invest Ophthalmol Vis Sci 2019; 60: 1265-1274.
8) Wang Z, Xiong L, Wang G, Wan W, Zhong C, Zu H. Insulin-like growth factor-1 protects SH-SY5Y cells against beta-amyloid-induced apoptosis via the PI3K/Akt-Nrf2 pathway. Exp Gerontol 2017; 87: 23-32.

9) McCubrey JA, Fitzgerald TL, Yang LV, Lertpiriyapong K, Steelman LS, Abrams SL, Montalto G, Cervello M, Neri LM, Cocco L, Martelli AM, Laidler P, Dulinska-Litewka J, Rakus D, Gizak A, Nicoletti F, Falzone L, Candido S, Libra M. Roles of GSK-3 and microRNAs on epithelial mesenchymal transition and cancer stem cells. Oncotarget 2017; 8: 14221-14250.

10) Wu C, Liu Z, Ma L, Pei C, Qin L, Gao N, Li J, Yin Y. MiRNAs regulate oxidative stress related genes via binding to the 3' UTR and TATA-box regions: a new hypothesis for cataract pathogenesis. BMC Ophthalmol 2017; 17: 142.

11) Salehi Z, Gholaminia M, Gholaminia Z, Panjtanpanah M, Qazvini MG. [The GG genotype of the HSPA1B gene is associated with increased risk of glaucoma in northern Iran]. Mol Biol (Mosk) 2017; 51: 31-36.

12) Lu Q, Hao M, Wu W, Zhang N, Isaac AT, Yin J, Zhu X, Du L, Yin X. Antidiabetic cataract effects of GbE, rutin and quercetin are mediated by the inhibition of oxidative stress and polyol pathway. Acta Biochim Pol 2018; 65: 35-41.

13) Bharathidevi SR, Babu KA, Jain N, Muthukumaran S, Umashankar V, Biswas J, Angayarkanni N. Ocular distribution of antioxidant enzyme paraoxonase & its alteration in cataractous lens; diabetic retina. Indian J Med Res 2017; 145: 513-520.

14) Pena-Blanco A, Garcia-Saez AJ. Bax, Bak and beyond - mitochondrial performance in apoptosis. FEBS J 2018; 285: 416-431.

15) Andreu-Fernandez V, Sancho M, Genoves A, Lucendo E, Todt F, Lauterwasser J, Funk K, Jahreis G, Perez-Paya E, Mingarro I, Edlich F, Orzaez M. Bax transmembrane domain interacts with prosurvival Bcl-2 proteins in biological membranes. Proc Natl Acad Sci U S A 2017; 114: 310-315.

16) Wang S, Zhou J, Kang W, Dong Z, Wang H. Tocilizumab inhibits neuronal cell apoptosis and activates STAT3 in cerebral infarction rat model. Bosn J Basic Med Sci 2016; 16: 145-150.

17) Li M, Peng J, Wang MD, Song YL, Mei YW, Fang Y. Passive movement improves the learning and memory function of rats with cerebral infarction by inhibiting neuron cell apoptosis. Mol Neurobiol 2014; 49: 216-221.

18) Butler DE, Marlein C, Walker HF, Frame FM, Mann VM, Simms MS, Davies BR, Collins AT, Maitland NJ. Inhibition of the PI3K/AKT/mTOR pathway activates autophagy and compensatory Ras/Raf/MEK/ERK signalling in prostate cancer. Oncotarget 2017; 8: 56698-56713.

19) Asati V, Mahapatra DK, Bharti SK. PI3K/Akt/mTOR and Ras/Raf/MEK/ERK signaling pathways inhibitors as anticancer agents: structural and pharmacological perspectives. Eur J Med Chem 2016; 109: 314-341.

20) Koh SH, Lo EH. The role of the PI3K pathway in the regeneration of the damaged brain by neural stem cells after cerebral infarction. J Clin Neurol 2015; 11: 297-304.

21) Wang H, Zhang C, Xu L, Zang K, Ning Z, Jiang F, Chi H, Zhu X, Meng Z. Bufalin suppresses hepatocellular carcinoma invasion and metastasis by targeting HIF-1alpha via the PI3K/AKT/mTOR pathway. Oncotarget 2016; 7: 20193-20208.

22) Yang X, Song X, Wang X, Liu X, Peng Z. Down-regulation of TM7SF4 inhibits cell proliferation and metastasis of A549 cells through regulating the PI3K/AKT/mTOR signaling pathway. Mol Med Rep 2017; 16: 6122-6127.

23) Baek SH, Ko JH, Lee JH, Kim C, Lee H, Nam D, Lee J, Lee SG, Yang WM, Um JY, Sethi G, Ahn KS. Ginkgolic acid inhibits invasion and migration and TGF-beta-induced EMT of lung cancer cells through PI3K/Akt/mTOR inactivation. J Cell Physiol 2017; 232: 346-354.

24) Zhang B, Liu XX, He JR, Zhou CX, Guo M, He M, Li MF, Chen GQ, Zhao Q. Pathologically decreased miR-26a antagonizes apoptosis and facilitates carcinogenesis by targeting MTDH and EZH2 in breast cancer. Carcinogenesis 2011; 32: 2-9.

25) Ichikawa T, Sato F, Terasawa K, Tsuchiya S, Toi M, Tsujimoto G, Shimizu K. Trastuzumab produces therapeutic actions by upregulating miR-26a and miR-30b in breast cancer cells. PLoS One 2012; 7: e31422.

26) Cui C, Xu G, Qiu J, Fan X. Up-regulation of miR-26a promotes neurite outgrowth and ameliorates apoptosis by inhibiting PTEN in bupivacaine injured mouse dorsal root ganglia. Cell Biol Int 2015; 39: 933-942.